MOL #91314

A Novel Pathway for Arsenic Elimination: Human Multidrug Resistance Protein 4 (MRP4/*ABCC4*) Mediates Cellular Export of Dimethylarsinic Acid (DMA^V) and the Diglutathione Conjugate of Monomethylarsonous acid (MMA^{III}).

Mayukh Banerjee, Michael W. Carew, Barbara A. Roggenbeck, Brayden D. Whitlock, Hua Naranmandura, X. Chris Le and Elaine M. Leslie

Department of Physiology *(MB, MWC, BAR, BDW, EML)*, Membrane Protein Disease Research Group *(MB, MWC, BAR, BDW, EML)*, Department of Laboratory Medicine and Pathology, Division of Analytical and Environmental Toxicology *(XCL, EML),* University of Alberta, Edmonton, AB, Canada. Institute of Pharmacology and Toxicology and Biochemical Pharmaceutics, Zhejiang University, Hangzhou, China *(HN).*

MOL #91314

Running Title: MRP4 protects cells from arsenic by exporting DMA^V and MMA(GS)$_2$.

Corresponding author: Elaine M. Leslie, 7-08A Medical Science Building, Department of Physiology, University of Alberta, Edmonton, Alberta, Canada, Tel: +1 780 492 9250, Fax: +1 780 492 8915, Email: eleslie@ualberta.ca

Text pages: 24

Tables: 4

Figures: 9

References: 61

Abstract: 249 words

Introduction: 751 words

Discussion: 1515 words

Supplemental Figures: 2

Non-standard abbreviations: ABC, ATP-binding cassette; As3MT, arsenic (+3 oxidation state) methyl transferase; As$_2$O$_3$, arsenic trioxide; As^{III}, arsenite; As^V, arsenate; As(GS)$_3$, arsenic triglutathione; BSO, L-buthionine sulfoximine; DMA^{III}, dimethylarsinous acid; DMA^V, dimethylarsinic acid; DMA(GS), dimethylarsenic glutathione; GSH, glutathione; ICP-MS, inductively coupled plasma mass spectrometry; LTC$_4$; leukotriene C$_4$, MMA^{III}, monomethylarsonous acid; MMA(GS)$_2$, monomethylarsenic diglutathione; MMA^V, monomethylarsonic acid; 6-MP, 6-mercaptopurine; MRP, multidrug resistance protein.

Abstract

Hundreds of millions of people world-wide are exposed to unacceptable levels of arsenic in drinking water. This is a public health crisis because arsenic is a Group I (proven) human carcinogen. Human cells methylate arsenic to monomethylarsonous acid (MMA^{III}), monomethylarsonic acid (MMA^{V}), dimethylarsinous acid (DMA^{III}), and dimethylarsinic acid (DMA^{V}). Although the liver is the predominant site for arsenic methylation, elimination occurs mostly in urine. The protein(s) responsible for transport of arsenic from the liver (into blood), ultimately for urinary elimination are unknown. Human multidrug resistance protein 1 (MRP1/*ABCC1)* and MRP2 *(ABCC2),* are established arsenic efflux pumps, but unlike the related MRP4 (*ABCC4*), are not present at the basolateral membrane of hepatocytes. MRP4 is also found at the apical membrane of renal proximal tubule cells making it an ideal candidate for urinary arsenic elimination. In the current study, human MRP4 expressed in HEK293 cells reduced the cytotoxicity and cellular accumulation of As^{V}, MMA^{III}, MMA^{V}, DMA^{III}, and DMA^{V} while two other hepatic basolateral MRPs (MRP3 and MRP5) did not. Transport studies with MRP4-enriched membrane vesicles revealed that the diglutathione conjugate of MMA^{III} [MMA(GS)$_2$] and DMA^{V} were the transported species. MMA(GS)$_2$ and DMA^{V} transport was osmotically sensitive, allosteric (Hill coefficients of 1.4 ± 0.2 and 2.9 ± 1.2, respectively), and high affinity (K$_{0.5}$ of 0.70 ± 0.16 µM and 0.22 ± 0.15 µM, respectively). DMA^{V} transport was pH dependent with highest affinity and capacity at pH 5.5. These results suggest human MRP4 could be a major player in the elimination of arsenic.

INTRODUCTION

It is estimated that 160 million people worldwide are exposed to arsenic through contaminated drinking water at levels above the World Health Organization guidelines of <10 ppb (Hubaux et al., 2013). Arsenic is classified as a Group I (proven) human carcinogen and causes skin, lung, and bladder tumors (IARC, 2012). Chronic arsenic exposure is also associated with kidney, liver, and prostate cancers and a myriad of other adverse health effects (IARC, 2012; Naujokas et al., 2013). Thus, arsenic is a major worldwide public health issue. In addition to environmental exposures, arsenic trioxide (As_2O_3) has been approved for treating both newly diagnosed and relapsed acute promyelocytic leukemia, and is under investigation for the treatment of multiple other haematological and solid tumors (Kritharis et al., 2013).

Contamination of drinking water occurs primarily from leaching of mineral bound arsenic and release of water soluble arsenate (As^V) and arsenite (As^{III}). As^V is chemically similar to inorganic phosphate and enters cells through the sodium/phosphate cotransporter type IIb (*SLC34A2*) (Villa-Bellosta and Sorribas, 2010). In solution, As^{III} and As_2O_3 exist as the neutral $As(OH)_3$, which passively enters cells through aquaglyceroporins (Yang et al., 2012). Arsenic is methylated within most mammalian cells. The most generally well accepted methylation pathway involves the enzymatic reduction of pentavalent arsenic followed by the oxidative methylation of trivalent species (Cullen, 2014). These reactions result in the consecutive formation of monomethylarsonic acid (MMA^V), monomethylarsonous acid (MMA^{III}), dimethylarsinic acid (DMA^V), and dimethylarsinous acid (DMA^{III}). In addition to methylation, As^{III} and MMA^{III} form conjugates with glutathione (GSH/GS) [$As(GS)_3$ and $MMA(GS)_2$, respectively] *in vivo,* while $DMA^{III}(GS)$ has never been isolated physiologically (Kala et al., 2004; Kala et al., 2000; Leslie, 2012).

Arsenic methylation occurs predominantly in the liver and increases the rate of arsenic clearance from the body (Drobna et al., 2010). Despite this, methylation is considered an activation pathway because MMA^{III} and DMA^{III} are substantially more toxic than As^{III} (Mass et al., 2001; Petrick et al., 2000). Arsenic elimination occurs predominantly in urine (60-80%), and of this, 10-30% is eliminated as inorganic arsenic, 10-20% as monomethylated, and 60-80% as dimethylated forms (Loffredo et al., 2003; Vahter, 2000). How arsenic species traverse the basolateral membrane of the hepatocyte to enter sinusoidal blood (ultimately for elimination in urine) is not well understood. To prevent and treat As-induced toxicity from either environmental or clinical exposures it is critical to understand underlying molecular mechanisms that render a person susceptible. This requires a thorough understanding of arsenic elimination pathways.

The multidrug resistance proteins (MRPs) are ATP-binding cassette (ABC) transporter proteins critical for the cellular efflux of a vast array of endogenous compounds, drugs, carcinogens, and environmental toxicants (Cole, 2013; Deeley et al., 2006; Keppler, 2011; Leslie et al., 2005). MRP1 *(ABCC1)* plays an important role in the cellular efflux of As(GS)$_3$ and MMA(GS)$_2$ (Carew et al., 2011; Leslie et al., 2004). *In vivo* studies of Mrp2 *(Abcc2)*-deficient (TR$^-$) Wistar rats show Mrp2 is responsible for the biliary excretion of As(GS)$_3$ and MMA(GS)$_2$ (Kala et al., 2000). As(GS)$_3$ and the seleno-bis(*S*-glutathionyl) arsinium ion [(GS)$_2$AsSe]$^-$ are substrates for human MRP2 *in vitro* (Carew and Leslie, 2010). Despite the important roles MRP1 and MRP2 play in protecting cells and tissues from arsenic, neither protein is localized to the basolateral surface of human hepatocytes. Thus, MRP1 and MRP2 are not responsible for the transport of hepatic arsenic metabolites into sinusoidal blood, ultimately for urinary elimination.

Candidate MRPs that are expressed at the basolateral surface of hepatocytes include

MRP3 (*ABCC3*), MRP4 (*ABCC4*) and MRP5 (*ABCC5*). MRP3-5 are not capable of reducing the cytotoxicity of inorganic arsenic (Kool et al., 1999; Lee et al., 2000; McAleer et al., 1999; Wijnholds et al., 2000); however, their ability to protect cells from methylated arsenic species is unknown. MRP4 is an ideal candidate for the urinary elimination of arsenic because it is localized at the basolateral surface of hepatocytes and the apical surface of renal proximal tubule cells (Russel et al., 2008). The objective of the current study was to determine the ability of HEK293 cells stably expressing MRP3, MRP4, or MRP5 to confer resistance to As^{III}, As^{V}, MMA^{III}, MMA^{V}, DMA^{III}, or DMA^{V} compared to cells expressing empty vector. MRP4 (but not MRP3 or MRP5) reduced the toxicity and accumulation of all arsenic species, except for As^{III}. MRP4-enriched membrane vesicles were then used to identify the transported species and determine transport characteristics. The results suggest that human MRP4 could be a major player in the elimination of arsenic from the human body.

MATERIALS AND METHODS

Materials. [3', 5', 7-^{3}H(N)]-methotrexate (13.4 Ci/mmol) was purchased from Moravek

Biochemicals Inc. (Brea, CA). GSH, ATP, AMP, sucrose, Tris base, As^{III} (>99% purity), As^V

(>98% purity), MMA^V (99.5% purity), DMA^V ($\geq$ 99%), L-buthionine sulfoximine (BSO) and

MgCl$_2$ were purchased from Sigma-Aldrich (Oakville, Ontario). Creatine kinase, glutathione

reductase, creatine phosphate, NADPH, and protease inhibitor cocktail tablets (Complete™, mini

EDTA free) were purchased from Roche Applied Science (Torrance, CA). Nitric acid was

purchased from Fisher Scientific (Ottawa, Ontario).   Ophthalmic acid (γ-Glutamyl-

Aminobutyryl-Glycine) was purchased from Bachem (Torrance, CA). MMA^{III} and DMA^{III} in

the form of diiodomethylarsine (CH$_3$AsI$_2$) and iododimethylarsine ([CH$_3$]$_2$AsI) were gifts from

Dr. William Cullen (University of British Columbia, BC, Canada). NMR analysis at the

University of British Columbia confirmed the identity of both chemicals and that the purity of

each was at least 99%.

Antibodies and Cell Lines. Mouse monoclonal (M$_3$II-9) anti-MRP3, rat monoclonal

(M$_4$I-10) anti-MRP4, and rat monoclonal (M$_5$-1) anti-MRP5 antibodies were purchased from

Abcam Inc (Cambridge, MA). The rabbit polyclonal (H-300) anti-Na$^+$/K$^+$ ATPase antibody was

purchased from Santa Cruz Biotechnology (Dallas, TX). The mouse monoclonal (QCRL1) anti-

MRP1 antibody was a gift from Dr. Susan Cole (Queen's University) (Hipfner et al., 1994). The

human embryonic kidney cell line (HEK293) and the SV40-transformed human embryonic

kidney cell like (HEK293T) were maintained in Dulbecco's modified Eagle's medium (DMEM)

supplemented with 4 mM L-glutamine and 7.5% FBS in a humidified incubator with 95% air/5%

CO$_2$. Routine testing for mycoplasma contamination of cell lines was performed using the

ATCC Universal Mycoplasma Testing Kit (Manassas, VA).

Generation of Expression Vectors and Stable HEK293 Cell Lines Expressing MRP3, MRP4 and MRP5. The pcDNA 3.1(+) MRP3 vector encoding the full length human MRP3 cDNA was a gift from Drs. Susan Cole and Roger Deeley (Queen's University, ON, Canada) and its construction has been described previously (Oleschuk et al., 2003). The pcDNA3.1(+)Hygro-MRP4 vector encoding the full length human MRP4 cDNA was a gift from Dr. Dietrich Keppler (German Cancer Research Center, Heidelberg, Germany) and was constructed as previously described (Rius et al., 2003). The MRP4 cDNA was excised from pcDNA3.1(+)Hygro-MRP4 vector using the restriction enzymes *NheI* and *XhoI*, and subcloned into pcDNA3.1(+)neomycin to generate pcDNA3.1(+)MRP4. The pGEM5-MRP5 vector containing the full length MRP5 cDNA was a gift from Dr. Piet Borst (The Netherlands Cancer Institute, Amsterdam, The Netherlands) (Kool et al., 1997). The MRP5 cDNA was excised from pGEM5-MRP5 using the restriction enzymes *EcoRI* and *HindIII,* and ligated into the pcDNA3.1(-) vector to generate pcDNA3.1(-) MRP5 (Invitrogen, Burlington, ON, Canada). All cloning sites and cDNA sequences were confirmed by sequencing (Macrogen USA, Rockville, MD).

For stable expression of MRP3, MRP4, MRP5, and empty pcDNA3.1(+), 2.5×10^5 HEK293 cells were seeded in each well of a 6 well plate, and 24 h later DNA (1 µg) was transfected using either FuGENE 6 transfection reagent (3µl) (according to the manufacturer's instructions) or the calcium phosphate transfection method [as described previously (Carew and Leslie, 2010)]. Forty-eight hours later, cells were subcultured (1:24) onto 6 well plates and medium was replaced with DMEM containing 1000 µg/ml G418 (Invitrogen) and 10% FBS. Cells were grown for ~2 weeks with regular media replacement, once cell colonies were visible, they were individually removed by scraping and aspirating with a pipette tip as described (Karin,

1999). Levels of MRP3, MRP4, and MRP5 in G418 resistant cell populations were then determined by immunoblot analysis with the anti-MRP3 MAb M_3II-9 (1:5000), anti-MRP4 MAb M_4I-10 (1:2000), and the anti-MRP5 MAb M_5I-1 (1:2000). The positive clones (MRP3-18, MRP4-1E16, and MRP5-2-6) and empty vector (V4) were tested for the proportion of cells expressing the MRP of interest by flow cytometry (BD FACS Calibur, Cross Cancer Institute) or confocal microscopy (Zeiss, 510 NLO, Cell Biology Imaging Facility, University of Alberta) as described previously (Leslie et al., 2003). Populations of less than 80% were further cloned by limiting dilution to obtain populations of >80%. Independently derived pcDNA3.1(+)Hygro and pcDNA3.1(+)Hygro-MRP4 stable cell clones (HEK-MCV and HEK-MRP4-MC4, respectively) were generated using HEK293T cells. Procedures used were identical to those described above except cells were selected and cultured in 100 μg/ml hygromycin (Invitrogen) instead of G418.

Cytotoxicity Testing. The cytotoxicity of six arsenic species was measured using HEK-V4, HEK-MRP3, HEK-MRP4-1E16, and HEK-MRP5 (G418 selected) or HEK-V-MC and HEK-MRP4-MC4 (hygromycin selected) stable cell lines, as previously described (Carew et al., 2011). Briefly, cells were seeded in 96-well plates at 1×10^4 cells/well and grown for 24h. In quadruplicate, cells were treated with As^{III} (0.1-100 μM), As^V (0.001-10 mM), MMA^{III} (0.1-100 μM), MMA^V (0.3-100 mM), DMA^{III} (0.1-100 μM), or DMA^V (0.01-100 mM) for 72 h. The pH of MMA^V and DMA^V was adjusted to pH 7.4 prior to treating cells. In parallel with arsenic species, the positive controls etoposide (0.1-100 μM) (for HEK-MRP3) and 6-mercaptopurine (6-MP) (0.1-100 μM) (for HEK-MRP4 and -MRP5) were run (Borst et al., 2007).

To measure the influence of GSH depletion on arsenic cytotoxicity, HEK-MRP4-1E16 and HEK-V4 cells were treated with buthionine sulfoximine (BSO, 100 μM), which inhibits the rate limiting step of GSH synthesis, at the time of seeding and for the remaining experimental

MOL #91314

duration. Cell viability was determined using the CellTiter96® AQueous Non-Radioactive Cell

Proliferation Assay (Promega) according to the manufacturer's instructions. Data were

analyzed and EC_{50} values determined using the sigmoidal dose response equation in Graphpad

Prism (GraphPad Software, San Diego, CA, USA). Relative resistance values were calculated as

the ratio of the EC_{50} values of HEK-MRP to HEK-vector.

Cellular Accumulation of Arsenic Species. HEK-MRP4-1E16 and HEK-V4 cells were

seeded in 6-well plates at 5×10^5 cells/well and 24 h later treated with 1 µM As^{III}, As^V, MMA^{III},

MMA^V, DMA^{III}, or DMA^V in culture media for 72 h.   Cells were then washed three times with

ice-cold phosphate buffered saline, trypsinized, pelleted by centrifugation at 1000 x g for 10 min

at 4ºC, and then digested with 250 µl concentrated nitric acid for >48 h. Digested cells were

diluted 1:1 with deionized distilled water and filtered through 0.45 µm syringe filters (Whatman,

Toronto, ON, Canada).   The total concentration of arsenic in samples was determined by

inductively coupled plasma mass spectrometry (ICP-MS) (Agilent 7500; Yokogawa Analytical

Systems, Hacchiouji, Japan) using the standard addition method, as described previously (Carew

et al., 2011; Kalivas, 1987).   Samples were introduced directly into the nebulizer of the ICP-MS.

Influence of As^{III}, MMA^{III}, DMA^{III} and DMA^V on MRP4 Protein Levels. HEK-V4 and

HEK-MRP4-1E16 cells were seeded in 75 cm^2 culture flasks at 2.5×10^6 cells/flask. Twenty-

four hours later, cells were treated with As^{III} (3.0 µM), MMA^{III} (1.5 µM), DMA^{III} (0.5 µM) or

DMA^V (750 µM) (concentrations at or below the EC_{50} value for HEK-V4 cells) for 72 h. Cells

were then harvested and crude membranes prepared.   Briefly, cells were washed twice in ice

cold Tris (50 mM, pH 7.4) sucrose (250 mM) buffer, and collected by centrifugation at 500 x g

for 10 min. Cell pellets were snap frozen in liquid nitrogen, thawed on ice and disrupted by

nitrogen cavitation (200 psi, 5 minutes) and the supernatant containing the membrane fraction

10

was collected following centrifugation at 500 x g for 10 minutes. Crude membrane fraction was

subsequently pelleted by centrifugation at 100,000 x g for 30 min, aliquoted and stored at -80°C.

MRP4 and MRP1 protein levels were then determined by immunoblot analysis using the rat anti-

human MRP4 antibody M_4-I10 (Abcam, Cambridge, MA) (1:2000) and the mouse anti-human

MRP1 antibody QCRL-1 (1:5000) after resolving 10 μg of protein by SDS-PAGE, as described

previously (Hipfner et al., 1994).

Transient Expression of MRP4 in HEK293T Cells and Membrane Vesicle Preparation.

HEK293T cells were transfected in 150 mm culture dishes using the calcium phosphate method,

as described previously (Carew and Leslie, 2010).   Twenty-four hours post transfection, culture

medium was replaced with fresh. Seventy-two hours post-transfection, cells were washed once

with Tris (50 mM, pH 7.4) sucrose (250 mM) buffer, scraped into 10 ml/plate of Tris sucrose

buffer and collected by centrifuging at 800 x g for 10 min. Cell pellets were stored at -80°C until

membrane vesicles were prepared. Plasma membrane-enriched vesicles were prepared from

MRP4 transfected HEK293T cells, according to previously described methods (Carew and

Leslie, 2010). MRP4 protein levels in membrane vesicles were determined by immunoblot

analysis, using the rat anti-human MRP4 antibody M_4-I10 (Abcam, Cambridge, MA) (1:2000).

Transiently expressed HEK293T cells were used for all membrane vesicle preparations because

MRP4 protein levels were ~2-fold higher after transient expression compared to the HEK-MRP4

stable cell lines (supplemental Figure 1).

MMA(GS)₂ and DMA^V Transport Assays. MMA(GS)$_2$ was synthesized from MMA[III]

and GSH as described previously (Kala et al., 2000; Carew et al., 2011). Briefly, MMA[III] (final

concentration of 50 μM) was combined with GSH (final concentration of 75 mM) in degassed

Tris sucrose buffer and incubated under a nitrogen atmosphere for >30 min at 4°C. Membrane

11

vesicles were incubated at 37ºC in Tris-sucrose buffer, with individual arsenic species (at

concentrations indicated), ATP or AMP (3.4 mM), MgCl$_2$ (8.5 mM), creatine kinase (85 µg/ml),

and creatine phosphate (8.5 mM). Conditions for the synthesis of MMA(GS)$_2$ resulted in the

presence of 3 mM GSH in the transport reaction. When GSH was present, GSH reductase (4.25

µg/ml) and NADPH (0.30 mM) were also included to convert oxidized to reduced GSH. GSH

dependence of MMA^{III} transport was assessed by adding GSH (3 mM) or the non-reducing GSH

analog ophthalmic acid (3 mM). At the indicated time point(s), transport was stopped by

diluting the transport reaction in 800 µl ice-cold Tris-sucrose buffer and pelleting vesicles by

centrifugation at 100,000 x g for 20 min at 4ºC.   Pelleted membrane vesicles were washed twice

with 1 ml ice-cold Tris-sucrose buffer, then digested in 250 µl concentrated nitric acid for 48 h,

diluted 1:1 with deionized distilled water, and filtered with 0.45 µm syringe filters (Whatman,

Toronto, ON).   The total concentration of arsenic in each sample was determined by ICP-MS,

using the standard addition method, as described previously (Carew et al., 2011; Kalivas, 1987).

ATP-dependent transport was determined by subtracting transport in the presence of AMP from

transport in the presence of ATP.

Kinetic parameters were determined by measuring the initial rate of MMA(GS)$_2$ and

DMA^{V} transport at 8 different substrate concentrations (0.07 - 6.7 µM) at a single time point of 3

and 5 min, respectively. Curve fitting was done by non-linear regression analysis (Michaelis

Menten curve fit or Allosteric Sigmoidal) with the computer program GraphPad Prism version 5

(GraphPad Software, San Diego, CA).

Methotrexate Transport Assay. Methotrexate transport by MRP4 was performed as

previously described (Chen et al., 2002; Li et al., 2011).   Briefly, 20 µg of membrane vesicles

were incubated with [^{3}H]methotrexate (1 µM, 200 nCi), AMP or ATP (4 mM), MgCl$_2$ (10 mM),

creatine phosphate (10 mM) and creatine kinase (100 µg/ml) at 37ºC for 5 min. Samples were

filtered over glass fiber filters and then radioactivity was quantified by liquid scintillation

counting. ATP-dependent transport was determined as described above for MMA(GS)$_2$ and

DMA^V.

RESULTS

MRP4 Confers Resistance to As^V, MMA^{III}, MMA^V, DMA^{III}, and DMA^V. To determine if MRP3, MRP4, and MRP5 were capable of conferring resistance to inorganic and methylated species of arsenic, stable HEK-MRP and HEK-vector cell lines were generated and treated with increasing concentrations of As^{III}, As^V, MMA^{III}, MMA^V, DMA^{III}, and DMA^V. The EC$_{50}$ value for each arsenical was determined and the relative resistance was calculated from the ratio of the EC$_{50}$ values for HEK-MRP and HEK-vector (summarized in Tables 1-3). Two independently derived HEK cell lines over-expressing MRP4 (HEK-MRP4-MC and HEK-MRP4-1E16) had similar expression levels (Figure 1A) and conferred low (1.5 to 3-fold), but significant levels of resistance to As^V, MMA^{III}, MMA^V, DMA^{III}, and DMA^V, compared to empty vector controls (Table 1 and Figure 1B-G). HEK-MRP4-1E16 conferred a 5-fold level of resistance to 6-MP (positive control) compared to HEK-V4 (Figure 1H and Table 1). MRP1 [a well characterized transporter of As(GS)$_3$ and MMA(GS)$_2$] was found at insignificant levels in the vector control and MRP4 over-expressing cell line pairs (Figure 1A).

HEK293 cells expressing MRP3 or MRP5 (expression levels shown in supplemental Figure 2) did not confer resistance to any of the arsenic species tested (Tables 2 and 3), compared with empty vector HEK-V4 cells. These cell lines conferred appropriate levels of resistance to either etoposide (positive control for MRP3) or 6-MP (positive control for MRP5) (Tables 2 and 3).

To determine whether resistance conferred by MRP4 to As^V, MMA^{III}, MMA^V, DMA^{III}, and DMA^V was GSH-dependent, toxicity was tested after depleting HEK-V4 and HEK-MRP4-

1E16 cells of GSH using BSO (100 µM).   GSH is protective against many arsenic species

(Leslie, 2012), and consistent with this, As^{III}, As^{V}, MMA^{V}, MMA^{III} and DMA^{V} became

significantly more toxic to both HEK-V4 and HEK-MRP4-1E16 cells upon depletion (Table 1

compared with Table 4). In contrast, GSH-depletion had no effect on the toxicity of DMA^{III}

(Table 1 compared with Table 4).   GSH depletion resulted in the loss of MRP4-dependant

cellular protection to As^{V} and MMA^{III}, but did not reduce the relative resistance for MMA^{V},

DMA^{III}, or DMA^{V} (Table 1 compared with Table 4).

MRP4 Reduces the Cellular Accumulation of Arsenic After Treatment with As^{V},

MMA^{III}, MMA^{V}, DMA^{III}, and DMA^{V}. To assess the effect of MRP4 on the cellular

accumulation of different arsenic species, total arsenic levels were quantified after HEK-V4 and

HEK-MRP4-1E16 cell treatment with As^{III}, As^{V}, MMA^{III}, MMA^{V}, DMA^{III}, and DMA^{V} (1 µM

for 72 h). HEK-MRP4-1E16 cellular accumulation of arsenic was reduced by 20%, 30%, 50%,

40% and 55% after treatment with As^{V}, MMA^{III} , MMA^{V}, DMA^{III}, and DMA^{V}, respectively,

compared with HEK-V4 cells (Figure 3). No significant difference in As^{III} accumulation

between HEK-MRP4-1E16 and HEK-V4 was observed (Figure 3). The accumulation of MMA^{V}

and DMA^{V} was 5-30-fold lower than any of the other arsenic species (Figure 3), consistent with

our high EC_{50} values, as well as previous studies suggesting these pentavalent methylated species

are inefficiently taken up by cells (Dopp et al., 2004; Naranmandura et al., 2007). Similar results

were obtained using the independently derived HEK-MCV and HEK-MRP4-MC4 cell line pair.

MRP4 Protein Expression is Increased by Certain Arsenic Species in HEK-V4 Cells.

To determine if selected arsenicals increase MRP4 protein expression in HEK-V4 and HEK-

MRP4-1E16 cell lines under conditions used for cytotoxicity and accumulation assays, MRP4

protein levels were measured after treating cells with concentrations of As^{III} (3 µM), MMA^{III} (1.5

MOL #91314

µM), DMA^{III} (0.5 µM) and DMA^{V} (750 µM) at or below the EC$_{50}$ value for the HEK-V4 cell line

(Table 1). For the HEK-V4 cell line, MRP4 protein was increased 1.9 to 2.5-fold by As^{III},

DMA^{III}, and DMA^{V} (Figure 4). In contrast, MRP4 protein levels were not significantly altered

for the MRP4 over-expressing HEK-MRP4-1E16 cell line. The influence of these conditions on

MRP1 protein levels was also tested (Figure 4A middle panel) and no significant level of MRP1

was detected in either cell line. These results suggest that MRP4 is induced by As^{III}, DMA^{III},

and DMA^{V} when cellular MRP4 levels are low. Similar results have been observed in sandwich

cultured human hepatocytes (Roggenbeck and Leslie, unpublished observation).

MRP4 Does Not Transport Inorganic Arsenic. HEK293 cells endogenously express the

enzyme responsible for the methylation of arsenic, arsenic (+3 oxidation state) methyl

transferase (As3MT) (Sumi et al., 2011). Thus, cytotoxicity and cellular accumulation data

(Figures 1-3 and Tables 1 and 4) provided evidence that MRP4 protects cells from arsenic

through cellular efflux, but did not identify the transported species. To identify the species of

arsenic that are substrates for MRP4, ATP-dependent transport of As^{III}, As^{V}, MMA^{III}, MMA^{V},

DMA^{III} and DMA^{V} (under various conditions and in the presence and absence of 3 mM GSH),

by MRP4-enriched and vector control membrane vesicles was measured. In contrast to the

cytotoxicity and accumulation data that suggested As^{V} was a GSH-dependent MRP4 substrate

(Figures 1B and 2B, Tables 1 and 4), MRP4 did not transport As^{V} in the presence or absence of

GSH (3 mM) (at As^{V} concentrations between 0.1-10 µM, time points ranging from 1-10 min, and

a pH range from 6-9) (data not shown). Consistent with the MTS and accumulation data, As^{III}

(0.1-10 µM) was not a substrate for MRP4 in the presence or absence of GSH (3 mM) or as the

triglutathione conjugate, As(GS)$_3$ (0.1-10 µM) (data not shown).

16

MRP4 Transports MMA[III] in the Presence of GSH or as the Presynthesized GSH Conjugate MMA(GS)₂. To determine whether MMA[III] and/or MMA(GS)$_2$ were substrates of MRP4, ATP-dependent transport of these compounds into MRP4-enriched and vector control membrane vesicles was measured (Fig 5A). ATP-dependant transport of MMA[III] by MRP4-enriched membrane vesicles was extremely low and similar to transport observed with the vector control membrane vesicles. In the presence of GSH (3 mM), ATP-dependent transport of MMA[III] was observed with an activity of 37 pmol mg^{-1} protein min^{-1}. Ophthalmic acid and other GSH analogs lacking a free thiol group can substitute for GSH and support the transport of GSH-dependent MRP substrates (Cole and Deeley, 2006). Thus, the thiol group of GSH and therefore the formation of a GSH conjugate are not necessary for transport. ATP-dependent transport of MMA[III] in the presence of ophthalmic acid (3 mM) was extremely low and similar to minus GSH conditions and vector control (Fig 5A). ATP-dependent transport of MMA(GS)$_2$ was then measured and had an activity of 39 pmol mg^{-1} protein min^{-1}. These data suggest that the free thiol group of GSH is required for MMA[III] transport by MRP4 and are consistent with MMA(GS)$_2$ being the transported chemical species. Using similar experimental conditions, transport of MMA[V] by MRP4 enriched membrane vesicles was measured, and ATP-dependent transport was not detected (data not shown).

Osmotic Sensitivity of MMA(GS)₂ Transport. To assess whether ATP-dependent transport of MMA(GS)$_2$ by MRP4-enriched membrane vesicles represents true transport into the vesicle lumen, rather than surface or intramembrane binding, the effect of changes in osmolarity on vesicular uptake was examined. MMA(GS)$_2$ (0.7 μM) uptake was decreased as the concentration of sucrose in the transport buffer increased, indicating that the ATP-dependent MMA(GS)$_2$ uptake by the vesicles is osmotically sensitive, as expected for a true transport

process (Figure 5B). Extrapolation of the line through X=0 (representing infinite osmolarity or zero intravesicular space) suggested that binding was ~20% for MRP4 under the usual transport conditions used.

Kinetic Analysis of MRP4-mediated MMA(GS)$_2$ Transport. To determine the linear range of MMA(GS)$_2$ (0.7 μM) uptake by MRP4-enriched and vector control membrane vesicles, time courses were completed. Transport by MRP4 was linear for up to 5 min with a maximal activity of 250 pmol mg^{-1} protein at 5 min (Figure 5C). ATP-dependent transport of MMA(GS)$_2$ by vector control membrane vesicles was very low and similar to transport observed in the presence of AMP. MRP4-mediated transport of MMA(GS)$_2$ was further characterized by determining the initial rates of transport over several concentrations of MMA(GS)$_2$ (Figure 5D). MRP4 showed a positive cooperative allosteric interaction with MMA(GS)$_2$. The curve fit for an allosteric interaction (allosteric sigmoidal equation, GraphPad Prism 5) was significantly better than a single binding site model (Michaelis-Menten equation, GraphPad Prism 5) (Extra sum of squares F test P<0.0001) with average (± S.D., *n=3*) $K_{0.5}$ of 0.70 ± 0.16 μM, V_{max} of 112 ± 6.3 pmol mg^{-1} protein min^{-1} and Hill coefficient of 1.4 ± 0.23.

MRP4 Transports DMA^V but not DMA^{III}. To determine if DMA^{III} was a substrate of MRP4, ATP-dependent transport of DMA^{III} (0.7 μM) in the presence or absence of GSH (3 mM) by MRP4-enriched membrane vesicles was measured (Figure 6). In the presence of GSH, transport was not detected and similar to transport observed in the presence of AMP (Figure 6A). However, in the absence of GSH, ATP-dependent transport of DMA^{III} was observed with an activity of 20 pmol mg^{-1} protein min^{-1} (Figure 6B). This was consistent with the resistance conferred to DMA^{III} by MRP4 under GSH-depleted conditions (Table 4 and Figure 2E). When dissolved at physiological pH, DMA^{III} is very unstable and rapidly oxidizes to DMA^V (Gong et

MOL #91314

al., 2001; Yehiayan et al., 2009). We hypothesized that DMA^{III} was not transported by MRP4 (+ GSH) because DMA^V is the transported species and GSH stabilizes DMA^{III} in its reduced state. To test this hypothesis, transport was measured after pre-incubating DMA^{III} dissolved in transport buffer for 1 or 10 min, to allow oxidation to DMA^V. Transport of DMA^{III}, incubated for 10 min prior to addition to the transport reaction, was 5-fold higher (25 pmol mg^{-1} protein min^{-1}) than DMA^{III} incubated for 1 min prior (5.0 pmol mg^{-1} protein min^{-1}) (Figure 6B). These data suggested that DMA^V, and not DMA^{III}, was the transported species. DMA^V transport was then measured using MRP4-enriched and vector control membrane vesicles. MRP4 transported DMA^V in an ATP-dependent manner with an activity of 18 pmol mg^{-1} protein min^{-1} while transport of DMA^V by vector control vesicles was not detectable (Figure 6C). Consistent with the GSH-independent resistance MRP4 conferred against DMA^V in cytotoxicity assays (Figure 2F and Table 4), the addition of GSH (3 mM) did not alter MRP4-dependent transport of DMA^V (Figure 6C).

Osmotic Sensitivity of DMA^V Transport. To assess whether ATP-dependent transport of DMA^V by MRP4-enriched membrane vesicles represents true transport into the vesicle lumen, rather than surface or intramembrane binding, the effect of changes in osmolarity on vesicular uptake was examined. DMA^V (0.7 μM) uptake was decreased as the concentration of sucrose in the transport buffer increased, indicating that the ATP-dependent DMA^V uptake by the vesicles is osmotically sensitive, as expected for a true transport process (Figure 7A). Extrapolation of the line through X=0 (representing zero intravesicular space) suggested very little ATP-dependent binding is occurring.

Kinetic Analysis of MRP4-mediated DMA^V Transport. To determine the linear range of DMA^V (0.7 μM) uptake by MRP4-enriched and vector control membrane vesicles, time courses

19

were completed. Transport by MRP4 was linear for up to 5 min with a maximal activity of 104

pmol mg^{-1} protein at 5 min (Figure 7B). ATP-dependent transport of DMA^V by vector control

membrane vesicles was very low and similar to transport observed in the presence of AMP.

MRP4-mediated transport of DMA^V was further characterized by determining the initial rates of

transport over several concentrations of DMA^V (Figure 7C). As for MMA(GS)$_2$, MRP4 showed

a positive cooperative allosteric interaction with DMA^V. The curve fit for an allosteric

interaction (allosteric sigmoidal equation, GraphPad Prism 5) was significantly better than a

single binding site model (Michaelis-Menten equation, GraphPad Prism 5) (Extra sum of squares

F test, P<0.0001) with average ($\pm$ S.D., $n=3$) K$_{0.5}$ of 0.22 $\pm$ 0.15 µM, V$_{max}$ of 32 $\pm$ 3 pmol mg^{-1}

protein min^{-1} and Hill coefficient of 2.9 $\pm$ 1.2.

   MRP4 Transport of DMA^V is pH Dependent. DMA^V [(CH$_3$)$_2$AsO$_2$H] is a weak acid

with a pKa of 6.3. To determine if pH influenced MRP4-dependent transport of DMA^V,

transport by MRP4-enriched membrane vesicles was measured at pH 5.5, 6.5, and 7.4 at which

the dissociated anion [(CH$_3$)$_2$AsO$_2^-$] would exist at 14%, 61%, and 93%, respectively. DMA^V

transport was highest at pH 5.5 with an activity of 38 pmol mg^{-1} protein min^{-1}, and similar at pH

6.5 and 7.5 with activities of 14 and 18 pmol mg^{-1} protein min^{-1}, respectively (Figure 8A). In

contrast with DMA^V, MMA(GS)$_2$ and methotrexate transport by MRP4 were not pH dependent

(Figure 8 B and C). For MMA(GS)$_2$, the dissociation constants for GSH (pKa for the carboxyl

groups 2.12 and 3.59) and the amino group (pKa 8.75) determine a predominant (>95%) net

charge of -2 over the pH range tested. For methotrexate, the dissociation constants of the γ-

carboxyl (pKa 4.7), α-carboxyl (pKa 3.4), and N(1) of the pteridine ring (pKa 5.7) determine the

net charge. Thus, at pH 5.5, 6.4, and 7.5 $\geq$ 61%, 86%, and 98%, respectively, of methotrexate

would have a net charge of -2 (with 39%, 14% and 2%, respectively at a net negative charge of -

1 due to the protonation of the pteridine ring) (Breedveld et al., 2007).

To further characterize the high level of DMA^V transport at pH 5.5, kinetic parameters

were determined (Figure 8D). Data were fit to the allosteric sigmoidal equation (GraphPad

Prism 5) with average (± S.D., *n=3*) $K_{0.5}$ of 0.073 ± 0.018 µM, V_{max} of 50 ± 2.3 pmol mg^{-1}

protein min^{-1}, and Hill coefficient value of 2.6 ± 0.3. Thus, the higher transport rate of DMA^V at

pH 5.5, compared with pH 7.4, results from a 3-fold reduction in the $K_{0.5}$ and a 1.6-fold increase

in the V_{max}, while the positively cooperative nature is similar.

DISCUSSION

We report for the first time that MRP4 is a high affinity transporter of the major urinary arsenic metabolite DMA^V, and the diglutathione conjugate of the highly toxic MMA^{III} [$MMA(GS)_2$]. This data along with the localization of MRP4 at the basolateral and apical surfaces of hepatocytes and renal proximal tubule cells, respectively, suggests MRP4 could be a major player in the elimination of arsenic from the human body. Two other hepatic basolateral MRPs, MRP3 and MRP5, did not confer resistance to any of the arsenic species tested, suggesting they are not involved in arsenic handling (summarized in Figure 9).

Stable expression of MRP4 in HEK293 cells resulted in reduced toxicity and cellular accumulation of all arsenic species tested, except for As^{III}. As^V is rapidly reduced to As^{III} once inside the cell, and prior to the first step of methylation, thus it was surprising that MRP4 conferred resistance to As^V, but not As^{III}. This observation was consistent with a previous report that MRP4 expressed in NIH3T3 cells did not confer resistance to As^{III} (Lee et al., 2000) and our finding that As^{III} ($\pm$ GSH) and $As(GS)_3$ were not substrates for MRP4. As^{III} is more toxic to cells than As^V (Tables 1-4) (Yang et al., 2012). Cellular uptake of As^{III} occurs at a faster rate than As^V (Yang et al., 2012), and this potentially results in the saturation of methylation pathways, impeding the formation of $MMA(GS)_2$ and DMA^V, and preventing MRP4 from playing a protective role.

Although MRP4 reduced the toxicity and cellular accumulation of As^V, MMA^V, and DMA^{III}, they were not transported by MRP4. MRP4 resistance to As^V was completely GSH-dependent suggesting MRP4 reduced the toxicity and accumulation of As^V by effluxing $MMA(GS)_2$. In contrast, MRP4 protected cells from MMA^V independently of GSH likely due to further methylation and efflux as DMA^V. Similar to MMA^V, MRP4 likely decreased DMA^{III}

toxicity and accumulation through the efflux of DMA^V. The relative resistance levels conferred

by MRP4 to MMA^V, DMA^{III} and DMA^V were increased after GSH-depletion (Table 1 compared

to Table 4), providing further support that MRP4 reduced the toxicity and cellular accumulation

of MMA^V and DMA^{III} through the efflux of DMA^V. DMA^V can be reduced to DMA^{III} through

an enzymatic and GSH-dependent process (Nemeti and Gregus, 2013) and GSH-depletion would

be protective because it would decrease the formation of highly toxic DMA^{III}, and allow the

efflux of DMA^V.

HEK-V4 cells treated with As^{III}, DMA^{III} and DMA^V had a 2- to 2.5-fold higher

expression of MRP4 than untreated cells. HEK293 cells methylate arsenic and the induction of

MRP4 by As^{III} could be indirect, through the production of a methylated arsenic species.

Alternatively, As^{III} could directly upregulate MRP4 expression, in preparation for the export of

$MMA(GS)_2$ and DMA^V. Arsenic is known to activate the arylhydrocarbon receptor (AhR) and

the nuclear factor (erythroid-derived 2)-like 2 (Nrf2), transcription factors critical for protecting

cells from oxidative stress (Kann et al., 2005; Lau et al., 2013). MRP4 mRNA and protein levels

are known to be induced through AhR and Nrf2 in primary human hepatocytes and HepG2 cells

(Xu et al., 2010), offering a possible mechanism by which arsenic induces MRP4.

The reduction in cellular toxicity and accumulation of arsenic species by MRP4 was low

and in seeming contrast to the transport data showing that $MMA(GS)_2$ and DMA^V are excellent

substrates for MRP4 (Figure 5D and 7C). Induction of endogenous MRP4 in the HEK-vector

cell line by arsenic offers a partial explanation; however, the HEK-MRP4-1E16 cell line still had

>10-fold more MRP4 than the induced HEK-V4 (Figure 4). It is likely that during these assays

the arsenic species effluxed by MRP4 are taken back up by the cell and exert toxicity again prior

to being re-effluxed. Thus, cytotoxicity and accumulation assays are likely an underestimation

of the *in vivo* situation where $MMA(GS)_2$ and DMA^V effluxed into the blood or proximal tubule lumen would be cleared from the tissue and the reuptake of arsenical prevented.

To our knowledge, DMA^V transport by MRP4 is the first pentavalent arsenic efflux pathway to be reported. Despite the highly reducing environment of the cell, DMA^V is detected in murine liver homogenates and human cell lines analyzed with oxidation state specific hydride generation-cryotrapping-atomic absorption spectroscopy (HG-CT-AAS) (Currier et al., 2011). Furthermore, the highly reactive nature of DMA^{III} combined with the lack of evidence for physiological formation of DMA(GS) (Leslie, 2012), means DMA^{III} is highly bound to protein and not available for transport (Hippler et al., 2011; Shen et al., 2013). MRP4 transport of DMA^V was with high apparent affinity ($K_{0.5}$ 0.22 µM) and would allow for the efficient efflux of DMA^V at low cellular concentrations. Although DMA^V is often regarded as a "non-toxic" arsenic species, the efflux of DMA^V from the cell and ultimately the body is critical to prevent the formation of the highly reactive and toxic DMA^{III}. In addition, efflux of DMA^V from the cell/body by MRP4 could prevent product inhibition of As3MT, allowing the formation and elimination of more DMA^V.

Similar to the transport of DMA^V, MRP4-mediated $MMA(GS)_2$ transport was with high apparent affinity ($K_{0.5}$ of 0.70 µM). These two newly identified MRP4 substrates have affinities comparable to the highest affinity MRP4 substrates reported to date, including the cysteinyl leukotriene, LTC_4 (K_m 0.1-0.3 µM) (Russel et al., 2008). The high affinity transport of DMA^V and $MMA(GS)_2$ is physiologically relevant for chronic environmental and clinical exposure to arsenic. Pharmacokinetic studies of patients undergoing chemotherapy for acute promyelocytic leukemia with As_2O_3 have plasma levels in the low µM range (Yoshino et al., 2009).

Environmental exposure would be approximately 100-fold lower with expected tissue levels in the 100 nM range (Kritharis et al., 2013).

The allosteric nature of $MMA(GS)_2$ and DMA^V transport by MRP4 was not surprising because the transport of other MRP4 substrates (urate and cGMP) is also through a positively co-operative mechanism (Van Aubel et al., 2005). The Hill coefficients for DMA^V of 2.9 ± 1.2 (pH 7.4) and 2.6 ± 0.3 (pH 5.5) are the highest reported to date for MRP4 (Hill coefficients for urate, cGMP and $MMA(GS)_2$ are 1.7, 1.4 and 1.4, respectively) suggesting DMA^V transport is mediated with strong positive co-operativity.   Transport of toxic substances from cells through an allosteric mechanism is extremely useful because it allows a rapid increase in the initial rate of transport with small increases in the concentration of toxicant.

In contrast with methotrexate and $MMA(GS)_2$, DMA^V was found to be transported by MRP4 in a pH dependent manner. The highest transport rate of DMA^V was at pH 5.5, at which the predominant form of DMA^V is neutral. In contrast, the transport rate of DMA^V at pH 6.5 and 7.4 did not correlate with the concentration of neutral or negatively charged species.   Thus, from the current data it is not possible to determine if the neutral, negatively charged or both forms of DMA^V are the substrate(s) for MRP4. MRP4 generally transports negatively charged molecules (Keppler, 2011; Russel et al., 2008), and transport of a neutral molecule would be somewhat unexpected.

Rat Mrp2 transports $As(GS)_3$ and $MMA(GS)_2$ into bile and this is potentially important for preventing hepatotoxicty; however, these GSH conjugates are not stable at the alkaline pH of bile (Gailer et al., 2002; Kala et al., 2000; Raab et al., 2004; Yehiayan et al., 2009). This leads to their rapid dissociation, reabsorption across the intestine and cycling back to the liver through the portal circulation (Dietrich et al., 2001; Suzuki et al., 2001). Therefore, biliary excretion of

As(GS)$_3$ and MMA(GS)$_2$ does not necessarily represent elimination of arsenic from the body (Leslie, 2012). In contrast, basolateral efflux of DMA^V and MMA(GS)$_2$ by MRP4 from the liver into sinusoidal blood could be a critical step in the pathway to eventual urinary elimination.

The localization of MRP4 to the apical surface of renal proximal tubule cells suggests that this protein might be important for the elimination of MMA(GS)$_2$ and DMA^V into urine. MRP2 is also found at the apical surface of the renal proximal tubule; however, studies using Mrp2-deficient TR$^-$ rats suggest that an Mrp in addition to Mrp2 is critical for urinary arsenic elimination (Kala et al., 2004).   In fact, the urinary elimination of total arsenic was increased approximately 2-fold in the absence of Mrp2, likely due to the loss of Mrp2-dependent enterohepatic circulation of As(GS)$_3$ and MMA(GS)$_2$ (Kala et al., 2004). A further explanation for the increased urinary elimination is the increased expression of Mrp4 in the kidney of the TR$^-$ rat (Chen et al., 2005). Overall, this evidence suggests that MRP4 could play a more important role in urinary arsenic elimination than MRP2.

To prevent and treat arsenic-induced toxicity, and to use arsenic effectively and safely in the clinic, it is critical to understand the cellular handling and elimination pathways of this metalloid. This work identifies MRP4 as a novel transport pathway for DMA^V and MMA(GS)$_2$. MRP4 is highly polymorphic (Abla et al., 2008; Krishnamurthy et al., 2008), and variants that alter DMA^V and/or MMA(GS)$_2$ transport could modulate an individual's susceptibility to arsenic-induced toxicity. The contribution of MRP4 to the well-established, but poorly understood inter-individual susceptibility to arsenic is worthy of future investigation.

ACKNOWLEDGEMENTS

MOL #91314

AUTHORSHIP CONTRIBUTIONS

Participated in research design: Carew, Banerjee, Roggenbeck, Whitlock, Leslie

Conducted experiments: Banerjee, Carew, Roggenbeck, Whitlock

Contributed new reagents or analytic tools: Carew, Roggenbeck, Naranmandura, Le

Performed data analysis: Banerjee, Carew, Roggenbeck, Whitlock, and Leslie

Wrote or contributed to the writing of the manuscript: Carew, Banerjee, Roggenbeck, and Leslie

REFERENCES

Abla N, Chinn LW, Nakamura T, Liu L, Huang CC, Johns SJ, Kawamoto M, Stryke D, Taylor TR, Ferrin TE, Giacomini KM and Kroetz DL (2008) The human multidrug resistance protein 4 (MRP4, ABCC4): functional analysis of a highly polymorphic gene. *J Pharmacol Exp Ther* **325**(3):859-868.

Borst P, de Wolf C and van de Wetering K (2007) Multidrug resistance-associated proteins 3, 4, and 5. *Pflugers Arch* **453**(5):661-673.

Breedveld P, Pluim D, Cipriani G, Dahlhaus F, van Eijndhoven MA, de Wolf CJ, Kuil A, Beijnen JH, Scheffer GL, Jansen G, Borst P and Schellens JH (2007) The effect of low pH on breast cancer resistance protein (ABCG2)-mediated transport of methotrexate, 7-hydroxymethotrexate, methotrexate diglutamate, folic acid, mitoxantrone, topotecan, and resveratrol in *in vitro* drug transport models. *Mol Pharmacol* **71**(1):240-249.

Carew MW and Leslie EM (2010) Selenium-dependent and -independent transport of arsenic by the human multidrug resistance protein 2 (MRP2/ABCC2): implications for the mutual detoxification of arsenic and selenium. *Carcinogenesis* **31**(8):1450-1455.

Carew MW, Naranmandura H, Shukalek CB, Le XC and Leslie EM (2011) Monomethylarsenic diglutathione transport by the human multidrug resistance protein 1 (MRP1/ABCC1). *Drug Metab Dispos* **39**(12):2298-2304.

Chen C, Slitt AL, Dieter MZ, Tanaka Y, Scheffer GL and Klaassen CD (2005) Up-regulation of Mrp4 expression in kidney of Mrp2-deficient TR⁻ rats. *Biochem Pharmacol* **70**(7):1088-1095.

Chen Z-S, Lee K, Walther S, Raftogianis RB, Kuwano M, Zeng H and Kruh GD (2002) Analysis of methotrexate and folate transport by multidrug resistance protein 4 (ABCC4): MRP4 is a component of the methotrexate efflux system. *Cancer Res* **62**:3144-3150.

Cole SP (2014) Targeting Multidrug Resistance Protein 1 (MRP1, ABCC1): Past, Present, and Future. *Annu Rev Pharmacol Toxicol*. **54**: 95-117.

Cole SP and Deeley RG (2006) Transport of glutathione and glutathione conjugates by MRP1. *Trends Pharmacol Sci* **27**(8):438-446.

Cullen WR (2014) Chemical mechanism of arsenic biomethylation. *Chem Res Toxicol* **27**(4):457-461.

Currier JM, Svoboda M, de Moraes DP, Matousek T, Dedina J and Styblo M (2011) Direct analysis of methylated trivalent arsenicals in mouse liver by hydride generation-cryotrapping-atomic absorption spectrometry. *Chem Res Toxicol* **24**(4):478-480.

Deeley RG, Westlake C and Cole SP (2006) Transmembrane transport of endo- and xenobiotics by mammalian ATP-binding cassette multidrug resistance proteins. *Physiol Rev* **86**(3):849-899.

Dietrich CG, Ottenhoff R, de Waart DR and Oude Elferink RP (2001) Role of MRP2 and GSH in intrahepatic cycling of toxins. *Toxicology* **167**(1):73-81.

Dopp E, Hartmann LM, Florea AM, von Recklinghausen U, Pieper R, Shokouhi B, Rettenmeier AW, Hirner AV and Obe G (2004) Uptake of inorganic and organic derivatives of arsenic associated with induced cytotoxic and genotoxic effects in Chinese hamster ovary (CHO) cells. *Toxicol Appl Pharmacol* **201**(2):156-165.

Drobna Z, Walton FS, Harmon AW, Thomas DJ and Styblo M (2010) Interspecies differences in metabolism of arsenic by cultured primary hepatocytes. *Toxicol Appl Pharmacol* **245**(1):47-56.

Gailer J, Madden S, Buttigieg GA, Denton MB and Younis HS (2002) Identification of $[(GS)_2AsSe]^-$ in rabbit bile by size-exclusion chromatography and simultaneous multielement-specific detection by inductively coupled plasma atomic emission spectroscopy. *Appl Organometal Chem* **16**:72-75.

Gong Z, Lu X, Cullen WR and Le XC (2001) Unstable trivalent arsenic metabolites, monomethylarsonous acid and dimethylarsinous acid. *Journal of Analytical Atomic Spectrometry* **16**(12):1409-1413.

Hipfner DR, Gauldie SD, Deeley RG and Cole SP (1994) Detection of the M(r) 190,000 multidrug resistance protein, MRP, with monoclonal antibodies. *Cancer Res* **54**:5788-5792.

Hippler J, Zdrenka R, Reichel RAD, Weber DG, Rozynek P, Johnen G, Dopp E and Hirnera AV (2011) Intracellular, time-resolved speciation and quantification of arsenic compounds in human urothelial and hepatoma cells. *J Anal At Spectrom* **26**:2396-2403.

Hubaux R, Becker-Santos DD, Enfield KS, Rowbotham D, Lam S, Lam WL and Martinez VD (2013) Molecular features in arsenic-induced lung tumors. *Mol Cancer* **12**:20.

IARC [International Agency for Research on Cancer] (2012) A review of human carcinogens: Arsenic, Metals, Fibres and Dusts. Lyon: World Health Organization Press.

Kala SV, Kala G, Prater CI, Sartorelli AC and Lieberman MW (2004) Formation and urinary excretion of arsenic triglutathione and methylarsenic diglutathione. *Chem Res Toxicol* **17**(2):243-249.

Kala SV, Neely MW, Kala G, Prater CI, Atwood DW, Rice JS and Lieberman MW (2000) The MRP2/cMOAT transporter and arsenic-glutathione complex formation are required for biliary excretion of arsenic. *J Biol Chem* **275**(43):33404-33408.

Kalivas JH (1987) Evaluation of volume and matrix effects for the generalized standard addition method. *Talanta* **34**(11):899-903.

Kann S, Huang MY, Estes C, Reichard JF, Sartor MA, Xia Y and Puga A (2005) Arsenite-induced aryl hydrocarbon receptor nuclear translocation results in additive induction of phase I genes and synergistic induction of phase II genes. *Mol Pharmacol* **68**(2):336-346.

Karin NJ (1999) Cloning of transfected cells without cloning rings. *Biotechniques* **27**(4):681-682.

Keppler D (2011) Multidrug resistance proteins (MRPs, ABCCs): importance for pathophysiology and drug therapy. *Handb Exp Pharmacol*(201):299-323.

Kool M, de Haas M, Scheffer GL, Scheper RJ, van Eijk MJ, Juijn JA, Baas F and Borst P (1997) Analysis of expression of cMOAT (MRP2), MRP3, MRP4, and MRP5, homologues of the multidrug resistance-associated protein gene (MRP1), in human cancer cell lines. *Cancer Res* **57**(16):3537-3547.

Kool M, van der Linden M, de Haas M, Scheffer GL, de Vree JM, Smith AJ, Jansen G, Peters GJ, Ponne N, Scheper RJ, Elferink RP, Baas F and Borst P (1999) MRP3, an organic anion transporter able to transport anti-cancer drugs. *Proc Natl Acad Sci U S A* **96**(12):6914-6919.

Krishnamurthy P, Schwab M, Takenaka K, Nachagari D, Morgan J, Leslie M, Du W, Boyd K, Cheok M, Nakauchi H, Marzolini C, Kim RB, Poonkuzhali B, Schuetz E, Evans W, Relling M and Schuetz JD (2008) Transporter-mediated protection against thiopurine-induced hematopoietic toxicity. *Cancer Res* **68**(13):4983-4989.

Kritharis A, Bradley TP and Budman DR (2013) The evolving use of arsenic in pharmacotherapy of malignant disease. *Ann Hematol* **92**(6):719-730.

MOL #91314

Lau A, Whitman SA, Jaramillo MC and Zhang DD (2013) Arsenic-mediated activation of the Nrf2-Keap1 antioxidant pathway. *J Biochem Mol Toxicol* **27**(2):99-105.

Lee K, Klein-Szanto AJ and Kruh GD (2000) Analysis of the MRP4 drug resistance profile in transfected NIH3T3 cells. *J Natl Cancer Inst* **92**(23):1934-1940.

Leslie EM (2012) Arsenic-glutathione conjugate transport by the human multidrug resistance proteins (MRPs/ABCCs). *J Inorg Biochem* **108**:141-149.

Leslie EM, Deeley RG and Cole SP (2005) Multidrug resistance proteins: role of P-glycoprotein, MRP1, MRP2, and BCRP (ABCG2) in tissue defense. *Toxicol Appl Pharmacol* **204**(3):216-237.

Leslie EM, Haimeur A and Waalkes MP (2004) Arsenic transport by the human multidrug resistance protein 1 (MRP1/ABCC1). Evidence that a tri-glutathione conjugate is required. *J Biol Chem* **279**(31):32700-32708.

Leslie EM, Letourneau IJ, Deeley RG and Cole SP (2003) Functional and structural consequences of cysteine substitutions in the NH_2-proximal region of the human multidrug resistance protein 1 (MRP1/ABCC1). *Biochemistry* **42**(18):5214-5224.

Li L, Sham YY, Bikadi Z and Elmquist WF (2011) pH-Dependent transport of pemetrexed by breast cancer resistance protein. *Drug Metab Dispos* **39**(9):1478-1485.

Loffredo CA, Aposhian HV, Cebrian ME, Yamauchi H and Silbergeld EK (2003) Variability in human metabolism of arsenic. *Environ Res* **92**(2):85-91.

Mass MJ, Tennant A, Roop BC, Cullen WR, Styblo M, Thomas DJ and Kligerman AD (2001) Methylated trivalent arsenic species are genotoxic. *Chem Res Toxicol* **14**(4):355-361.

McAleer MA, Breen MA, White NL and Matthews N (1999) pABC11 (also known as MOAT-C and MRP5), a member of the ABC family of proteins, has anion transporter activity but does not confer multidrug resistance when overexpressed in human embryonic kidney 293 cells. *J Biol Chem* **274**(33):23541-23548.

Naranmandura H, Ibata K and Suzuki KT (2007) Toxicity of dimethylmonothioarsinic acid toward human epidermoid carcinoma A431 cells. *Chem Res Toxicol* **20**(8):1120-1125.

Naujokas MF, Anderson B, Ahsan H, Aposhian HV, Graziano JH, Thompson C and Suk WA (2013) The broad scope of health effects from chronic arsenic exposure: update on a worldwide public health problem. *Environ Health Perspect* **121**(3):295-302.

Nemeti B and Gregus Z (2013) Reduction of dimethylarsinic acid to the highly toxic dimethylarsinous acid by rats and rat liver cytosol. *Chem Res Toxicol* **26**(3):432-443.

Oleschuk CJ, Deeley RG and Cole SP (2003) Substitution of Trp1242 of TM17 alters substrate specificity of human multidrug resistance protein 3. *Am J Physiol Gastrointest Liver Physiol* **284**(2):G280-289.

Petrick JS, Ayala-Fierro F, Cullen WR, Carter DE and Vasken Aposhian H (2000) Monomethylarsonous acid (MMA(III)) is more toxic than arsenite in Chang human hepatocytes. *Toxicol Appl Pharmacol* **163**(2):203-207.

Raab A, Meharg AA, Jaspars M, Genney DR and Feldmann J (2004) Arsenic-glutathione complexes-their stability in solution and during separation by different HPLC modes. *J Anal At Spectrom* **19**:183-190.

Rehman K and Naranmandura H (2012) Arsenic metabolism and thioarsenicals. *Metallomics* **4**(9):881-892.

Rius M, Nies AT, Hummel-Eisenbeiss J, Jedlitschky G and Keppler D (2003) Cotransport of reduced glutathione with bile salts by MRP4 (ABCC4) localized to the basolateral hepatocyte membrane. *Hepatology* **38**(2):374-384.

Russel FG, Koenderink JB and Masereeuw R (2008) Multidrug resistance protein 4 (MRP4/ABCC4): a versatile efflux transporter for drugs and signalling molecules. *Trends Pharmacol Sci* **29**(4):200-207.

Shen S, Li XF, Cullen WR, Weinfeld M and Le XC (2013) Arsenic binding to proteins. *Chem Rev* **113**(10):7769-7792.

Sumi D, Fukushima K, Miyataka H and Himeno S (2011) Alternative splicing variants of human arsenic (+3 oxidation state) methyltransferase. *Biochem Biophys Res Commun* **415**(1):48-53.

Suzuki KT, Tomita T, Ogra Y and Ohmichi M (2001) Glutathione-conjugated arsenics in the potential hepato-enteric circulation in rats. *Chem Res Toxicol* **14**(12):1604-1611.

Vahter M (2000) Genetic polymorphism in the biotransformation of inorganic arsenic and its role in toxicity. *Toxicol Lett* **112-113**:209-217.

Van Aubel RA, Smeets PH, van den Heuvel JJ and Russel FG (2005) Human organic anion transporter MRP4 (ABCC4) is an efflux pump for the purine end metabolite urate with multiple allosteric substrate binding sites. *Am J Physiol Renal Physiol* **288**(2):F327-333.

33

Villa-Bellosta R and Sorribas V (2010) Arsenate transport by sodium/phosphate cotransporter type IIb. *Toxicol Appl Pharmacol* **247**(1):36-40.

Wijnholds J, Mol CA, van Deemter L, de Haas M, Scheffer GL, Baas F, Beijnen JH, Scheper RJ, Hatse S, De Clercq E, Balzarini J and Borst P (2000) Multidrug-resistance protein 5 is a multispecific organic anion transporter able to transport nucleotide analogs. *Proc Natl Acad Sci U S A* **97**(13):7476-7481.

Xu S, Weerachayaphorn J, Cai SY, Soroka CJ and Boyer JL (2010) Aryl hydrocarbon receptor and NF-E2-related factor 2 are key regulators of human MRP4 expression. *Am J Physiol Gastrointest Liver Physiol* **299**(1):G126-135.

Yang HC, Fu HL, Lin YF and Rosen BP (2012) Pathways of arsenic uptake and efflux. *Curr Top Membr* **69**:325-358.

Yehiayan L, Pattabiraman M, Kavallieratos K, Wang X, Boise LH and Cai Y (2009) Speciation, formation, stability and analytical challenges of human arsenic metabolites. *J Anal At Spectrom* **24**:1397-1405.

Yoshino Y, Yuan B, Miyashita SI, Iriyama N, Horikoshi A, Shikino O, Toyoda H and Kaise T (2009) Speciation of arsenic trioxide metabolites in blood cells and plasma of a patient with acute promyelocytic leukemia. *Anal Bioanal Chem* **393**(2):689-697.

MOL #91314

FOOTNOTES

Mayukh Banerjee and Michael W. Carew contributed equally to the work.

Address correspondence to: Dr. Elaine M. Leslie, 7-08A Medical Sciences Building, Department of Physiology, University of Alberta, Edmonton, AB, Canada, T6G 2H7; Email: eleslie@ualberta.ca; Tel: (780) 492-9250; Fax: (780) 492-8915.

MOL #91314

FIGURE LEGENDS

Figure 1. Effect of As^{III}, As^{V}, MMA^{III}, MMA^{V}, DMA^{III} and DMA^{V} on the viability of stably transfected HEK293 cells. A) The relative levels of MRP4 in membrane vesicles (2 µg of protein) prepared from stably transfected HEK293 cells expressing pcDNA3.1(+)Hygro (MCV), pcDNA3.1(+)Hygro-MRP4 (MRP4-MC4), pcDNA3.1(+)neomycin (V4), or pcDNA3.1(+)MRP4 (MRP4-1E16) were determined after resolving protein by SDS-PAGE and immunoblotting with the MRP4 antibody M$_4$I-10. Blots were then stripped and probed for either MRP1 (using the MRP1 antibody QCRL-1) or the Na$^+$/K$^+$ ATPase as a loading control (using the Na$^+$/K$^+$ ATPase antibody H-300). B-H) Empty vector (HEK-V4) (○) and MRP4 (HEK-MRP4-1E16) (●) expressing cells were incubated in the presence of B) As^{III}, C) As^{V}, D) MMA^{III} E) MMA^{V}, F) DMA^{III}, G) DMA^{V} or H) 6-MP for 72 h. Cell viability was determined using a tetrazolium-based cytotoxicity assay. Data points are means (± S.D.) of quadruplicate determinations in a representative experiment; similar results were obtained in at least three additional experiments.

Figure 2. Effect of As^{III}, As^{V}, MMA^{III}, MMA^{V}, DMA^{III} and DMA^{V} on the viability of stably transfected HEK293 cells after glutathione depletion. HEK-V4 (○) and HEK-MRP4-1E16 (●) cells were incubated with 100 µM BSO for 24 h and then treated with 100 µM BSO and A) As^{III}, B) As^{V}, C) MMA^{III} D) MMA^{V}, E) DMA^{III} or F) DMA^{V} for 72 h. Cell viability was determined using a tetrazolium-based cytotoxicity assay. Data points are means (± S.D.) of quadruplicate determinations in a representative experiment; similar results were obtained in at least three additional experiments.

Figure 3. Accumulation of As^{III}, As^{V}, MMA^{III}, DMA^{III}, MMA^{V} and DMA^{V} by stably transfected HEK cells. HEK-V4 (open bars) and HEK-MRP4-1E16 (closed bars) cells were treated with 1 µM of (A) As^{III}, As^{V}, MMA^{III}, or DMA^{III} or (B) MMA^{V} or DMA^{V} for 72 h. Cells were then harvested and digested with nitric acid, and total arsenic was determined using ICP-MS. Bars represent the means of three independent experiments (±S.D.). *$P<0.05$ (Student's *t* test)

Figure 4. As^{III}, DMA^{III} and DMA^{V} increase MRP4 protein levels in HEK-V4 cells. A) Immunoblot analysis of crude membrane preparations (10 µg) isolated from HEK293 cells stably expressing empty pcDNA3.1(+) neomycin (HEK-V4) or pcDNA3.1(+)MRP4 (HEK-MRP4-1E16) and treated with As^{III} (3 µM), MMA^{III} (1.5 µM), DMA^{III} (0.5 µM) or DMA^{V} (750 µM) for 72 h. Blots were probed with the MRP4 antibody (M$_4$I-10), stripped and probed with the MRP1 antibody QCRL-1, and stripped and probed with the Na^{+}/K^{+} ATPase antibody (H-300). B) Densitometry on the MRP4 and Na^{+}/K^{+} ATPase bands was performed with ImageJ software. MRP4 levels were normalized for protein loading using the Na^{+}/K^{+} ATPase and plotted as a % of untreated control. Bars represent the mean ± S.D. values from three independent experiments. *$P<0.05$ (ANOVA followed by a Dunnett's multiple comparison post-hoc test).

Figure 5. ATP-dependent transport of MMA^{III} (± GSH or ophthalmic acid) and MMA(GS)$_2$ by MRP4-enriched membrane vesicles. Transport experiments were done with membrane vesicles (20 µg of protein) prepared from HEK293T cells transiently transfected with pcDNA3.1(+)MRP4 (closed bars or symbols) or empty pcDNA3.1(+) (open bars or symbols). A) Membrane vesicles were incubated in transport buffer for 3 min at 37ºC with MMA^{III} (1µM)

[either alone or in the presence of GSH (3 mM) or ophthalmic acid (OA) (3 mM)] or $MMA(GS)_2$

(1 µM). B) Osmotic sensitivity of ATP-dependent $MMA(GS)_2$ transport by MRP4 was

determined by incubating HEK-MRP4 membrane vesicles with $MMA(GS)_2$ (0.7 µM) for 3 min

at 37ºC in transport buffer containing increasing concentrations of sucrose (0.25, 0.33, 0.5, 0.67

and 1 M). C) Time course of ATP-dependent $MMA(GS)_2$ transport by MRP4 was determined

by incubating HEK-MRP4 membrane vesicles with $MMA(GS)_2$ (0.7 µM) in transport buffer at

37ºC for the indicated time points. D) HEK-MRP4 membrane vesicles were incubated for 3 min

at 37ºC with increasing concentrations of $MMA(GS)_2$ (0.07-6.7 µM). Data were fit using a one-

site Michaelis-Menten kinetic model (hatched line) or the allosteric sigmoidal model (solid line)

with GraphPad Prism 5. For individual experiments, transport was done in triplicate then

reactions were pooled for analysis by ICP-MS.   Bars and symbols represent the means of three

independent experiments (±S.D.), except in panel C where open symbols are means of two

independent experiments.

Figure 6. ATP-dependent transport of dimethylated arsenic species by MRP4-enriched

membrane vesicles. Transport experiments were done with membrane vesicles (20 µg of

protein) prepared from HEK293T cells transiently transfected with pcDNA3.1(+)MRP4 (closed

bars) or empty pcDNA3.1(+) (open bars). A) Vesicles were incubated for 5 min at 37ºC in

transport buffer with DMA^{III} in the presence or absence of GSH (3 mM). B) Vesicles were

incubated for 1 min at 37ºC in transport buffer with DMA^{III}, prepared 1 min or 10 min prior to

addition to transport reaction. C) Vesicles were incubated with DMA^V (0.7 µM) for 5 min at

37ºC, in the presence or absence of GSH (3 mM).   For individual experiments transport was

done in triplicate then reactions were pooled for analysis by ICP-MS.   Bars represent the means

of three independent experiments (± S.D.).

Figure 7. Osmotic sensitivity and kinetic analysis of MRP4-mediated ATP-dependent

transport of DMA^V. Transport experiments were done with membrane vesicles (20 µg of

protein) prepared from HEK293T cells transiently transfected with pcDNA3.1(+)MRP4 (closed

symbols) or empty pcDNA3.1(+) (open symbols). A) Osmotic sensitivity of ATP-dependent

DMA^V transport by MRP4 was determined by incubating HEK-MRP4 membrane vesicles with

DMA^V (0.7 µM) for 5 min at 37ºC in transport buffer containing increasing concentrations of

sucrose (0.25, 0.33, 0.5, 0.67 and 1 M). B) Time course of ATP-dependent DMA^V transport

was determined by incubating membrane vesicles with DMA^V (0.7 µM) in transport buffer at

37ºC for the indicated time points. C) HEK-MRP4 membrane vesicles were incubated for 5 min

at 37ºC with increasing concentrations of DMA^V (0.07-6.7 µM). Data were fit using a one-site

Michaelis-Menten kinetic model (hatched line) or the allosteric sigmoidal model (solid line) with

GraphPad Prism 5. For individual experiments, transport was done in triplicate then reactions

were pooled for analysis by ICP-MS.   Bars and symbols represent the means of three

independent experiments (±S.D.), except in panel B where open symbols are means of two

independent experiments.

Figure 8. Effect of pH on MRP4-mediated ATP-dependent transport of DMA^V,

MMA(GS)$_2$ and methotrexate. Transport experiments were done with membrane vesicles (20

µg of protein) prepared from HEK293T cells transiently transfected with pcDNA3.1(+)MRP4.

A) Membrane vesicles were incubated for 5 min at 37ºC with DMA^V (0.7 µM) at the indicated

pH.   B) Membrane vesicles were incubated for 3 min at 37ºC with $MMA(GS)_2$ (0.7 μM) at the

indicated pH. C) Membrane vesicles were incubated for 5 min at 37ºC with methotrexate (1

μM; 200 nCi) at the indicated pH. D) HEK-MRP4 membrane vesicles (20 μg of protein) were

incubated for 5 min at 37ºC with increasing concentrations of DMA^V (0.07-6.7 μM) at pH 5.5.

Data were fit using a one-site Michaelis-Menten kinetic model (hatched line) or the allosteric

sigmoidal model (solid line) with GraphPad Prism 5. (A, B and D) For individual experiments,

transport was done in triplicate then reactions were pooled for analysis by ICP-MS. Bars and

symbols represent the means of three independent experiments (± S.D.). (C) Bars represent the

mean (± S.D.) of triplicate determinations in a single experiment. Similar results were obtained

in two additional experiments.

Figure 9. Arsenic methylation/glutathionylation and transport by hepatic MRPs.

According to the classical arsenic methylation pathway pentavalent arsenic species are reduced

and then undergo oxidative methylation (Cullen, 2014). As^{III} and MMA^{III} can form GSH

conjugates [$As(GS)_3$ and $MMA(GS)_2$] which are effluxed from the hepatocyte into bile by the

apical MRP2 (Kala et al., 2000). The majority of arsenic is eliminated in urine and therefore

must cross the basolateral surface of the hepatocyte into sinusoidal blood for entry into the

systemic circulation. MRP3, MRP4 and MRP5 are in the correct location for this function, but

only MRP4 reduced the cytotoxicity of arsenic. MRP4 was found to transport $MMA(GS)_2$ and

DMA^V. According to the classical methylation pathway, efflux of DMA^V from the hepatocyte

would limit the formation of DMA^{III}. The GSH conjugate of DMA^{III} is indicated with a question

mark because it has never been identified physiologically (Kala et al., 2004; Kala et al., 2000).

This figure is not meant to be comprehensive and only selected aspects of arsenic cellular

handling are represented. For a recent comprehensive overview the reader is referred to

(Rehman and Naranmandura, 2012). Abbreviations: As(GS)$_3$, arsenic triglutathione; As^{III},

arsenite; As3MT, arsenic (+3 oxidation state) methyltransferase; As^V, arsenate; MRP, multidrug

resistance protein; DMA^{III}, dimethylarsinous acid; DMA^V, dimethylarsinic acid; DMA(GS),

dimethylarsenic glutathione; GSH, glutathione; MMA^{III}, monomethylarsonous acid; MMA^V,

monomethylarsonic acid; MMA(GS)$_2$, monomethylarsenic diglutathione.

TABLES

TABLE 1. Resistance of human MRP4 transfected HEK293 cells to inorganic and methylated arsenic species.

Arsenic Species	EC_{50} ($\pm$ S.D.) [a]		Relative Resistance[b]
	HEK-V4	HEK-MRP4-1E16	($\pm$ S.D.)
As^{III} (n = 6)	3.1 ± 0.8	2.7 ± 1.5	0.7 ± 0.3
As^{V} (n = 9)	20 ± 8.1	49 ± 15 *	2.9 ± 1.8
MMA^{III} (n =9)	1.7 ± 0.4	2.9 ± 0.5 *	1.7 ± 0.4
MMA^{V} (n = 4)	0.54 ± 0.08[c]	0.81 ± 0.14 [c] *	1.5 ± 0.1
DMA^{III} (n = 7)	0.7 ± 0.1	1.2 ± 0.2 *	2.0 ± 0.6
DMA^{V} (n = 8)	0.8 ± 0.1 [c]	1.2 ± 0.2 [c] *	1.6 ± 0.3
6-MP (n = 6)	5.1 ± 1.9	26 ± 5.8*	5.4 ± 1.4
	HEK-MCV	HEK-MRP4-MC4	
As^{III} (n = 5)	3.2 ± 1.1	3.9 ± 1.6	1.2 ± 0.2
As^{V} (n = 6)	31 ± 13	78 ± 18 **	3.0 ± 1.8
MMA^{III} (n =4)	0.7 ± 0.2	1.7 ± 0.1 **	2.9 ± 1.0
MMA^{V} (n = 3)	0.3 ± 0.1[c]	0.5 ± 0.1 [c] **	1.6 ± 0.7
DMA^{III} (n = 4)	0.6 ± 0.2	1.0 ± 0.4 **	1.9 ± 0.7
DMA^{V} (n = 3)	0.7 ± 0.02 [c]	1.2 ± 0.3 [c] **	1.6 ± 0.4

*EC_{50} for HEK-MRP4-1E16 is significantly different from HEK-V4, $P < 0.05$ (Student's t test).

**EC_{50} for HEK-MRP4-MC4 is significantly different from HEK-MCV, $P < 0.05$ (Student's t test).

[a]Values are given in µM unless otherwise indicated.

[b]Mean of the ratio of EC_{50}HEK-MRP4/ EC_{50} HEK-vector

[c]Values are given in mM

TABLE 2. Resistance of human MRP3 transfected HEK293 cells to inorganic and methylated arsenic species

	EC$_{50}$ ($\pm$ S.D.)[a]		Relative Resistance[b] ($\pm$ S.D.)
	HEK-V4	HEK-MRP3	
As^{III} (n =3)	5.5 $\pm$ 2.3	4.3 $\pm$ 1.6	0.8 $\pm$ 0.1
As^{V} (n = 4)	22 $\pm$ 7.9	34 $\pm$ 14	1.5 $\pm$ 0.2
MMA^{III} (n = 3)	1.5 $\pm$ 0.7	1.3 $\pm$ 0.3	0.9 $\pm$ 0.2
MMA^{V} (n = 3)	0.63 $\pm$ 0.1[c]	0.66 $\pm$ 0.03[c]	1.0 $\pm$ 0.2
DMA^{III} (n = 2)	0.5; 0.6	0.1; 0.7	0.3; 1.1
DMA^{V} (n = 3)	0.8 $\pm$ 0.1[c]	0.7 $\pm$ 0.1[c]	1.0 $\pm$ 0.1
Etoposide (n=8)	0.2 $\pm$ 0.1	1.3 $\pm$ 0.6*	6.9 $\pm$ 1.6

*EC$_{50}$ for HEK-MRP3 is significantly different from HEK-V4, $P < 0.05$ (Student's t test).

[a]Values are given in μM unless otherwise indicated.

[b]Mean of the ratio of EC$_{50}$HEK-MRP3/ EC$_{50}$ HEK-V4

[c]Values are given in mM

TABLE 3. Resistance of human MRP5 transfected HEK293 cells to inorganic and methylated arsenic species

	EC_{50} ($\pm$ S.D.)[a]		Relative Resistance[b]
	HEK-V4	HEK-MRP5	($\pm$ S.D.)
As^{III} ($n = 5$)	7.7 ± 2.8	7.4 ± 3	1.0 ± 0.4
As^{V} ($n = 3$)	33 ± 7.8	22 ± 5	0.7 ± 0.2
MMA^{III} ($n = 5$)	1.4 ± 0.5	1.7 ± 0.9	1.2 ± 0.4
MMA^{V} ($n = 3$)	0.62 ± 0.1[c]	0.55 ± 0.19[c]	0.9 ± 0.3
DMA^{III} ($n = 4$)	0.6 ± 0.2	0.8 ± 0.1	1.3 ± 0.5
DMA^{V} ($n = 6$)	1.1 ± 0.3[c]	0.9 ± 0.3[c]	0.7 ± 0.1
6-MP ($n = 8$)	3.3 ± 1.2	6.4 ± 1.5*	2.1 ± 0.8

*EC_{50} for HEK-MRP5 is significantly different from HEK-V4, $P < 0.05$ (Student's t test).

[a]Values are given in μM unless otherwise indicated.

[b]Mean of the ratio of EC_{50}HEK-MRP5/ EC_{50} HEK-V4

[c]Values are given in mM

TABLE 4. Resistance of human MRP4 transfected HEK293 cells to inorganic and methylated arsenic species after cellular GSH depletion

Arsenic Species	EC_{50} ($\pm$ S.D.) (μM)		Relative Resistance[a]
	HEK-V4	HEK-MRP4-1E16	
As^{III} (n = 5)	0.2 ± 0.01	0.23 ± 0.006	1.1 ± 0.02
As^{V} (n = 8)	2.9 ± 0.7	2.8 ± 0.5	0.9 ± 0.4
MMA^{III} (n = 7)	0.06 ± 0.04	0.06 ± 0.03	1.0 ± 0.5
MMA^{V} (n = 4)	85 ± 12	169 ± 6 *	2.0 ± 0.3
DMA^{III} (n = 5)	0.6 ± 0.1	1.9 ± 0.7 *	2.9 ± 0.5
DMA^{V} (n =4)	25.1 ± 1.1	62.4 ± 16 *	2.5 ± 0.8

*EC_{50} for HEK-MRP4 -1E16 is significantly different from HEK-V4, $P < 0.05$ (Student's t test).
[a]Mean of the ratio of EC_{50} HEK-MRP4-1E16/ EC_{50} HEK-V4

Figure 1

Figure 2

Figure 3

Figure 4

(A)

(B)

Figure 5

Figure 6

Figure 7

Figure 8

A

DMA^V transport (pmol mg^{-1} min^{-1}) vs pH (5.5, 6.5, 7.4)

B

MMA(GS)$_2$ transport (pmol mg^{-1} min^{-1}) vs pH (5.5, 6.5, 7.4)

C

Methotrexate transport (pmol mg^{-1} min^{-1}) vs pH (5.5, 6.5, 7.4)

D

DMA^V transport (pmol mg^{-1} min^{-1}) vs DMA^V (μM)

n=2.6

n=1
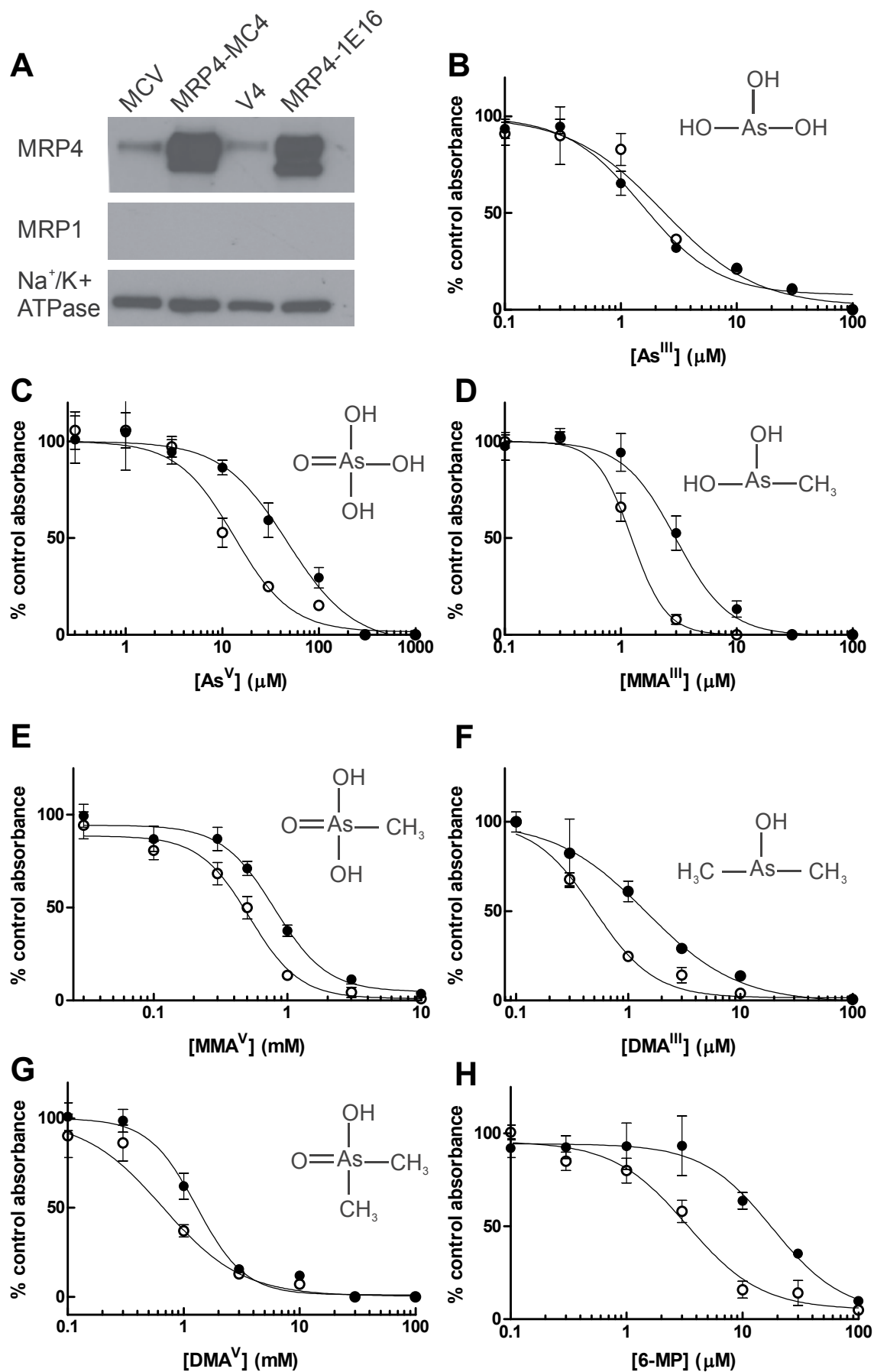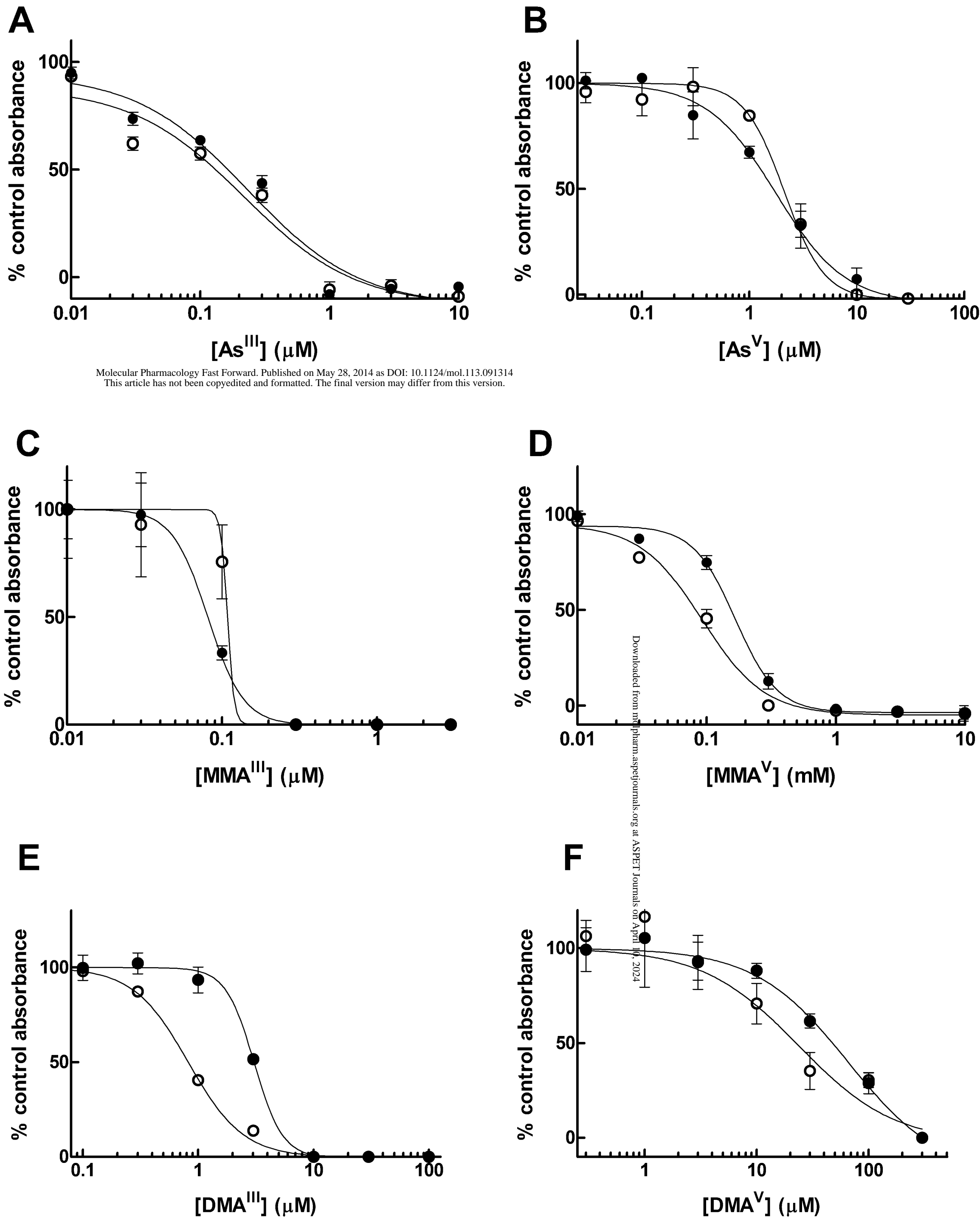
Figure 9.

MOLECULAR PHARMACOLOGY

Supplemental Data

A Novel Pathway for Arsenic Elimination: Human Multidrug Resistance Protein 4 (MRP4/*ABCC4*) Mediates Cellular Export of Dimethylarsinic Acid (DMA^{V}) and the Diglutathione Conjugate of Monomethylarsonous acid (MMA^{III}).

Mayukh Banerjee, Michael W. Carew, Barbara A. Roggenbeck, Brayden D. Whitlock, Hua Naranmandura, X. Chris Le and Elaine M. Leslie

Supplemental Figure 1. MRP4 and MRP1 protein levels in HEK293T transiently or HEK293 cells stably expressing MRP4.

Supplemental Figure 2. MRP3 and MRP5 protein levels after stable expression in HEK293 cells.
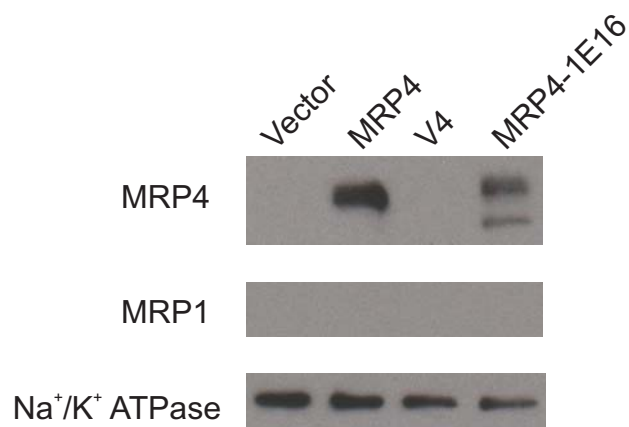
Supplemental Figure 1. MRP4 and MRP1 protein levels in HEK293T transiently or HEK293 cells stably expressing MRP4. MRP4 levels in membrane vesicles (2 µg of protein) prepared from HEK293T cells transiently expressing empty pcDNA3.1(+)neomycin (Vector) or pcDNA3.1(+)MRP4 (MRP4) and HEK293 cells stably expressing pcDNA3.1(+)neomycin (V4) or pcDNA3.1(+)MRP4 (MRP4-1E16) were determined after resolving protein by SDS-PAGE and immunoblotting with the MRP4 antibody M_4I-10. Blots were then stripped and probed for either MRP1 (using the MRP1 antibody QCRL-1) or the Na^+/K^+ ATPase as a loading control (using the Na^+/K^+ ATPase antibody H-300).
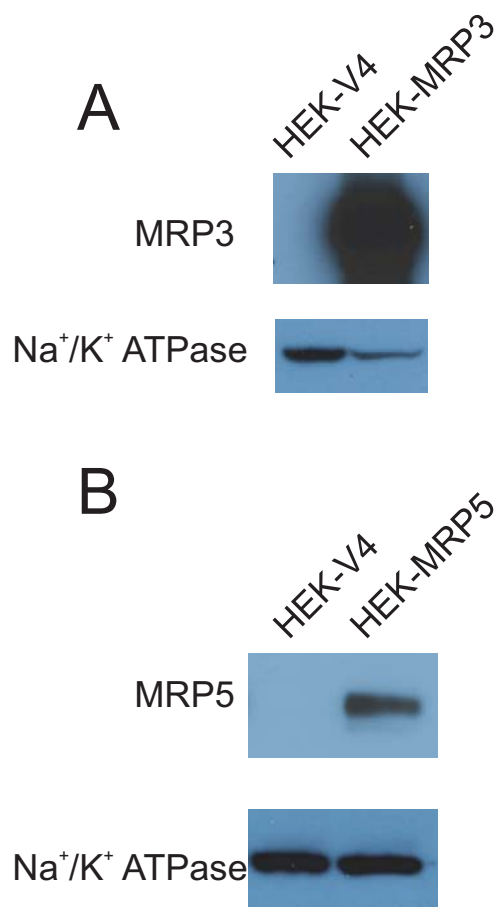
Supplemental Figure 2. MRP3 and MRP5 protein levels after stable expression in HEK293 cells. The relative levels of A) MRP3 or B)MRP5 in membrane vesicles (2 µg of protein) prepared from HEK293 cells stably expressing empty vector pcDNA3.1(+)neomycin (V4), pcDNA3.1(+)MRP3 (HEK-MRP3) or pcDNA3.1(-)MRP5 (HEK-MRP5). Protein was resolved by SDS-PAGE and blotted with either the MRP3 antibody M_3II-9 or the MRP5 antibody M_5I-1. Blots were then stripped and probed for the Na+/K+ ATPase as a loading control (using the Na^+/K^+ ATPase antibody H-300).